Available online at www.sciencedirect.com
ScienceDirect
Journal of Power Sources 159 (2006) 107–110
JOURNAL OF POWER SOURCES
www.elsevier.com/locate/jpowsour

Short communication

Catalytic activity of oxides and halides on hydrogen storage of MgH_2

V.V. Bhat [a], A. Rougier [a,*], L. Aymard [a], X. Darok [a], G. Nazri [b], J.M. Tarascon [a]

[a] *LRCS, 33 rue St. Leu, 80039 Amiens, France*
[b] *GM Research and Development Center, Warren, MI, United States*

Available online 30 May 2006

Abstract

Hydrogen sorption kinetics of ball milled MgH_2 with and without chemical additives were studied. We observed kinetics and capacity improvement with increasing the number of sorption cycles that contributed to the micro/nano cracking of MgH_2 particles, shown by XRD and SEM studies. In addition, to investigate the proposed specific role of O^{2-}-based additives on the sorption kinetics of MgH_2, we have undertaken a comparative study evaluating the performances of MgH_2 containing the $NbCl_5$, CaF_2 or Nb_2O_5 additives. At 300 °C, addition of $NbCl_5$ and CaF_2 improved the sorption capacity to 5.2 and 5.6 wt% within 50 min, respectively, in comparison to the required 80 min in the case of Nb_2O_5. This suggests the importance of the chemical nature of the catalyst for hydrogen sorption in MgH_2. In addition, the catalyst specific surface area was shown to be very critical. High surface area Nb_2O_5 (200 $m^2\ g^{-1}$), prepared by novel precipitation method, exhibits an excellent catalytic activity and helped to desorb 4.5 wt% of hydrogen from MgH_2 within 80 min at a temperature as low as 200 °C.

Keywords: Oxides; Halides; Magnesium hydride; Hydrogen sorption properties; Catalyst

1. Introduction

The high theoretical hydrogen storage capacity of MgH_2 (7.6 wt%) projects this compound as a viable material for hydrogen storage application for portable fuel cells aiming towards the development of future vehicles [1–3]. However, owing to both its slow sorption kinetics and too high operating temperatures (>375 °C for commercial MgH_2), this material is presently unsuitable for real on-road hydrogen storage uses [3–5]. Several approaches were pursued over the last few years to overcome this problem. For instance, improvement in sorption kinetics of MgH_2 is achieved either through ball-milling approach [6,7] or addition of catalysts such as carbon [7,8], transition metals [4,9] and transition metal oxides [10,11].

Among the catalysts, transition metal oxides present a better catalytic activity than their corresponding metal constituent [10,11], although the exact catalytic mechanism is not yet determined. It is argued that the oxygen content in the oxides plays an important role in catalyzing hydrogen desorption from MgH_2 [10,12]. To verify this point, we compared the effect of oxide catalyst, Nb_2O_5, with its halide counterpart $NbCl_5$ and also with a non transition metal halide such as CaF_2. We also explored the effect of high surface area Nb_2O_5-based catalyst prepared by precipitation technique. In this paper, the influence of the various catalysts on the sorption temperature and kinetics of ball milled MgH_2 is discussed.

2. Experimental

Five batches of 2 g of commercial MgH_2 ($(MgH_2)_{com}$) (from Aldrich, 95% MgH_2, 5% Mg) are milled under a 20 bar hydrogen pressure for 38 h in a stainless steel 50 ml-container using a Spex-8000. After ball-milling, all the batches were mixed together and milled again for 38 h, so that a larger batch of starting material with uniform properties could be used for catalyst addition studies. The sample is named $(MgH_2)_{bm}$.

Highly crystalline commercial Nb_2O_5 (c-Nb_2O_5) from Aldrich is used. To investigate the effect of surface area, the catalytic activities of c-Nb_2O_5 and high surface area Nb_2O_5, prepared by a novel precipitation route, are compared. To prepare an oxidizing medium, 2 g of $Na_2S_2O_8$ is added to the boiling solution of 1 g NaOH in 100 ml solution. Immediately after, 2 g $NbCl_5$ dissolved in 100 ml alcohol solution is added to the above boiling solution. The formed white precipitate is filtered and washed with distilled water till the precipitate free from Cl^- ions is obtained, and dried at 100 °C for 4 h to remove excess water. The surface area of the prepared material, termed here-

* Corresponding author. Tel.: +33 3 22 82 76 04; fax: +33 3 22 82 75 90.
E-mail address: aline.rougier@u-picardie.fr (A. Rougier).

0378-7753/$ – see front matter © 2006 Elsevier B.V. All rights reserved.
doi:10.1016/j.jpowsour.2006.04.059

after p-Nb_2O_5, was measured by BET technique using Gemini instrument.

$(MgH_2)_{bm}$ is mixed with 0.4 mol% commercial $NbCl_5$ (c-$NbCl_5$), 0.2 mol% c-Nb_2O_5, 0.4 mol% commercial CaF_2 (c-CaF_2) and 0.2 mol% p-Nb_2O_5, and milled for 2 h under argon atmosphere in a stainless steel container using Spex 8000. The samples are named as $(MgH_2)_{catalyst}$, where catalysts are c-$NbCl_5$, c-Nb_2O_5, c-CaF_2 and p-Nb_2O_5. Samples are characterized by X-ray diffraction (XRD) using a Philips diffractometer (θ–2θ configuration and λ (Cu Kα, 1.5418 Å)). Scanning electron microscopy (SEM) is carried out on Philips XL 30 field emission gun FEG microscope. The sorption properties are investigated using Hiden IGA thermobalance. Hydrogen absorption was performed under continuously increased pressure up to 15 bar and desorption was carried out under primary vacuum.

3. Results and discussion

3.1. Characterization of $(MgH_2)_{bm}$

The XRD patterns of $(MgH_2)_{com}$ and $(MgH_2)_{bm}$ are presented in Fig. 1. $(MgH_2)_{com}$ exhibits high intensity sharp X-ray diffraction peaks of β-MgH_2 (space group: $P4/_2mnm$), residual unreacted Mg impurity was also detected. The corresponding SEM micrographs show large grains of more than 50 μm in size. In contrast to $(MgH_2)_{com}$, $(MgH_2)_{bm}$ presents broad X-ray diffraction peaks of β-MgH_2 and the diffraction lines corresponding to the high pressure metastable γ-MgH_2 (space group: *Pbcn*) in a 85:15 ratio. Around 5% Fe impurity is also detected, which is due to the high energy ball milling in stainless steel container. SEM micrographs of $(MgH_2)_{bm}$ display agglomerates of small particles along with a few dispersed grains larger than 10 μm. Interestingly, despite the presence of large grains, $(MgH_2)_{bm}$ presents broad diffraction peaks. This indicates that the broadening of MgH_2 diffraction peaks is not only due to the agglomerates of fine particles, but also includes the strain contribution due to the high energy ball milling.

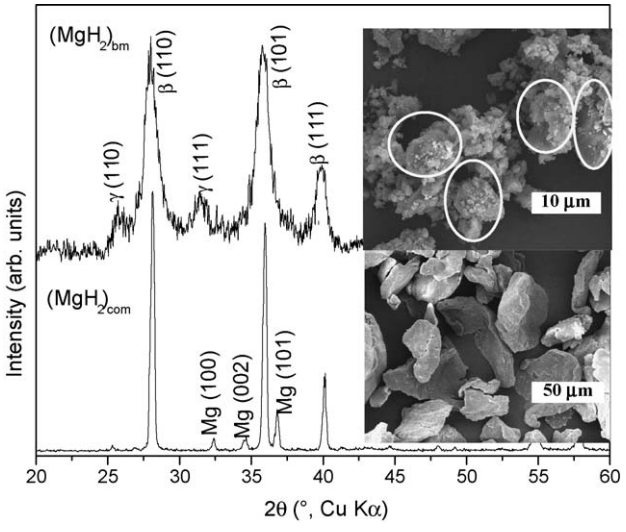

Fig. 1. X-ray diffraction patterns and SEM micrographs of commercial $(MgH_2)_{com}$ and ball milled $(MgH_2)_{bm}$.

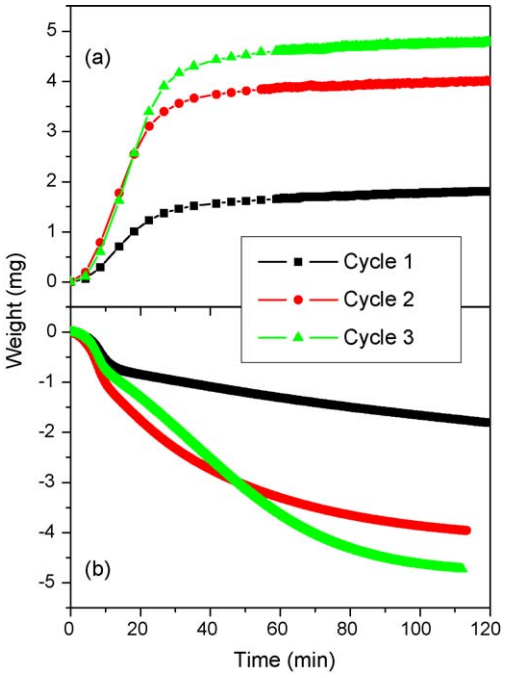

Fig. 2. Sorption behavior of $(MgH_2)_{bm}$ at 300 °C: (a) absorption under dynamic pressure increase up to 15 bar and (b) desorption under primary vacuum.

At 300 °C, the sorption cycling reveals that $(MgH_2)_{com}$ desorbs less than 0.5 wt% even after 100 min. Therefore, its sorption properties are not presented in this paper. Fig. 2a and b present sorption properties of $(MgH_2)_{bm}$ for different sorption cycles at 300 °C. During the first desorption cycle, $(MgH_2)_{bm}$ requires nearly 120 min for the desorption of 1.5 wt% hydrogen. During the second subsequent cycle, $(MgH_2)_{bm}$ desorbs nearly 3.8 wt% in 110 min. During the third cycle nearly 4.8 wt% hydrogen are desorbed within 110 min. This improvement in the desorption kinetics and capacity indicates that the activation of MgH_2 is induced by cycling due to the formation of smaller particle sizes. The enhancement of desorption rate with cycling was already reported by Liang et al. for $LaNi_5$-MgH_2 systems [13]. However, the cause for such activation is not addressed in the literature.

At 300 °C, $(MgH_2)_{bm}$ absorbs nearly 95% of hydrogen within 30 min under dynamic pressure increase conditions (Fig. 2a). The hydrogen absorption starts around 2500 mbar at 300 °C and ∼95% of absorption is completed around 7000 mbar. The amount of hydrogen absorbed in each cycle is equal to the amount of hydrogen desorbed in the previous cycle, showing a complete reversibility. The sorption cycling after the initial three cycles did not significantly change the absorption kinetics. However, the hydrogen storage capacity increased within the first three cycles. For the first cycle, 1.8 wt% of hydrogen is absorbed. In the consecutive cycles, the hydrogen absorption capacity increased from 3.8 to 4.8 wt%.

XRD patterns and SEM micrographs of $(MgH_2)_{bm}$-before and after cycling are presented in Fig. 3. The XRD of $(MgH_2)_{bm}$-before cycling presents broad diffraction peaks of β- and γ-MgH_2, and its SEM micrographs exhibit large MgH_2 particles dispersed in agglomerates of fine MgH_2 particles. Conversely, $(MgH_2)_{bm}$-after cycling shows only β-MgH_2 with traces of

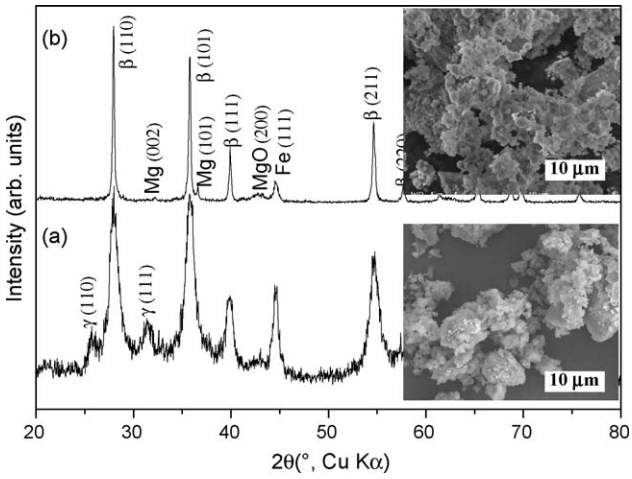

Fig. 3. X-ray diffraction patterns and SEM micrographs of $(MgH_2)_{bm}$ before and after cycling at 300 °C.

unreacted Mg and also Fe impurity. The X-ray diffraction peaks are sharp and intense compared to those of $(MgH_2)_{bm}$-before cycling. The SEM micrographs exhibit agglomerates of fine particles without any large particles, which were present before cycling.

The cause for improvement in rate and capacity with hydriding-dehydriding cycles is addressed in this part. The SEM micrographs and XRD patterns clearly show that $(MgH_2)_{bm}$ contains agglomerates of fine particles with high defect concentration. During desorption, MgH_2 loses hydrogen to form Mg. In this process, the unit-cell volume of MgH_2 is decreased by 25%. Due to the volume shrinkage and expansion during sorption cycles, MgH_2 particles undergo repeated breaking and downsizing. This hypothesis is confirmed by SEM micrographs of $(MgH_2)_{bm}$-after cycling, which do not show any large particles. However, the XRD pattern of $(MgH_2)_{bm}$-after cycling exhibits sharper intense peaks of β-MgH_2 with no trace of the γ phase. The sharpness of the β-MgH_2 X-ray peaks indicates that sorption cycling at 300 °C removes the lattice defects and forms the defect free thermodynamically stable β-MgH_2 phase.

3.2. Characterization of $(MgH_2)_{catalyst}$

Fig. 4 shows the desorption kinetics of $(MgH_2)_{bm}$, $(MgH_2)_{c\text{-}Nb_2O_5}$ $(MgH_2)_{c\text{-}NbCl_5}$ and $(MgH_2)_{c\text{-}CaF_2}$. Compared to $(MgH_2)_{bm}$, the desorption properties of all $(MgH_2)_{catalyst}$ are significantly enhanced by addition of the catalysts. $(MgH_2)_{c\text{-}Nb_2O_5}$ desorbs nearly 5.2 wt% hydrogen in 80 min. In contrast, $(MgH_2)_{c\text{-}NbCl_5}$ desorbs the same amount of hydrogen in 50 min and $(MgH_2)_{c\text{-}CaF_2}$ desorbs 5.8 wt% in 50 min. This shows that both transition and non transition metal halides have similar catalytic properties as the transition metal oxides.

To further understand the effect of surface area on desorption properties of MgH_2, the catalytic activity of p-Nb_2O_5 is compared to that of c-Nb_2O_5 at different temperatures (Fig. 5). We wish to note that p-Nb_2O_5, which exhibits 200 $m^2\ g^{-1}$ BET specific surface area, shows featureless XRD pattern indicating its amorphous nature. At 300 °C, $(MgH_2)_{c\text{-}Nb_2O_5}$ desorbs

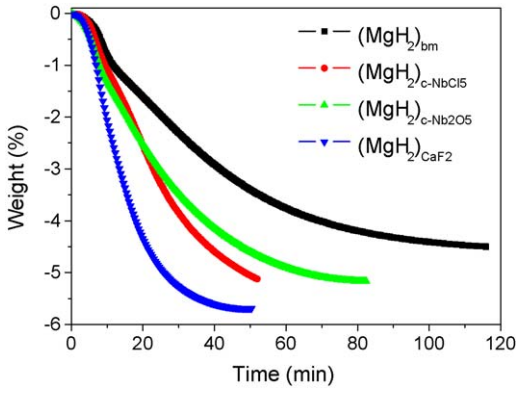

Fig. 4. Effect of various catalysts on the desorption behavior of $(MgH_2)_{catalyst}$.

5.2 wt% hydrogen in 80 min, in comparison to only 15 min for $(MgH_2)_{p\text{-}Nb_2O_5}$. This strong improvement in desorption kinetics shows that high surface area p-Nb_2O_5 acts as a better catalyst than the c-Nb_2O_5. Further lowering of the operating temperature to 250 °C decreases the desorption kinetics of both $(MgH_2)_{c\text{-}Nb_2O_5}$ and $(MgH_2)_{p\text{-}Nb_2O_5}$. From $(MgH_2)_{c\text{-}Nb_2O_5}$ only 2.5 wt% hydrogen could be desorbed in 100 min. However in $(MgH_2)_{p\text{-}Nb_2O_5}$, more than 5 wt% of hydrogen is desorbed in 35 min. At 200 °C, $(MgH_2)_{c\text{-}Nb_2O_5}$ does not exhibit any hydrogen desorption, but $(MgH_2)_{p\text{-}Nb_2O_5}$ shows nearly 4.5 wt% hydrogen desorption within 100 min. This shows that using p-Nb_2O_5, a significant amount of hydrogen could be desorbed even at 200 °C with moderately fast kinetics.

The better catalytic activity of Nb_2O_5, as compared with Nb metal in hydrogen sorption kinetics of MgH_2, is also reported in the literature [10,11]. These reports claim that a small amount of oxide catalysts results in a large improvement in the reaction kinetics but observe no significant effect from ultra pure

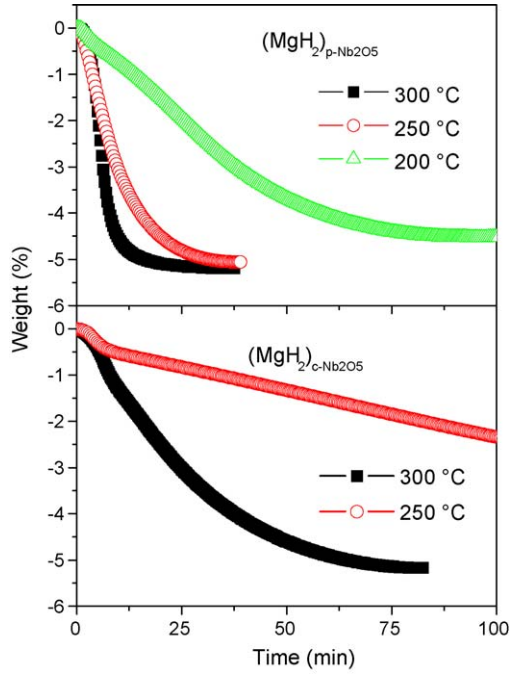

Fig. 5. Comparative sorption properties of $(MgH_2)_{c\text{-}Nb_2O_5}$ and $(MgH_2)_{p\text{-}Nb_2O_5}$.

metals like Nb or V. To understand the role of transition metal cations, Nb^{5+} and the anion O^{2-}, we performed hydrogen sorption of MgH_2 in the presence of $NbCl_5$ and CaF_2 catalysts. Surprisingly, both catalysts demonstrate a better catalytic activity compared to Nb_2O_5. The better catalytic activity of $NbCl_5$ indicates that the oxygen in Nb_2O_5 is not the key ion to enhance the kinetics. On the other hand, CaF_2 exhibits a better catalytic activity than Nb_2O_5, which reveals that Nb^{5+} is also not the only important ion that catalyzes the reaction. However, in all cases, using Nb_2O_5, CaF_2 and $NbCl_5$ catalyst significant size reduction was observed, indicating that particle size and morphology play an important role in improving the sorption kinetics of MgH_2. In addition, from these data, it can be also corroborated the importance of ionic nature of the catalyst in improving hydrogen sorption kinetics. However, the variation in the catalytic activity within a series of oxides or halides can be dependent on the constituent ions. It is clearly demonstrated that the high catalytic activity of the p-Nb_2O_5 with high surface area is superior to that of low surface area c-Nb_2O_5 indicating that the high surface area and morphology of the catalysts are important criteria in designing catalyst for hydriding–dehyriding of metal hydrides.

4. Conclusion

In this paper, the relevant parameters related to the use of MgH_2 as hydrogen storage material are addressed. The activation of ball milled MgH_2 upon sorption cycles, the chemical nature and the high surface area of the catalysts are proved to be important for hydrogen sorption. A significant improvement in the sorption kinetics is observed upon cycling. The disappearance of large particles and their conversion into fine powders reveal that the frequent volume changes during cycling lead to cracking and pulverisation of the material that improve the sorption kinetics.

The higher catalytic activity for $NbCl_5$ and CaF_2 as compared to the Nb_2O_5 was observed indicating that neither oxide ion nor transition metal cation are crucial for hydrogen sorption. However, the ionicity of the catalyst is proved to be important in enhancing the sorption process of MgH_2. Strong enhancement in the sorption kinetics and hydrogen storage capacity using high surface area p-Nb_2O_5 catalyst demonstrates the importance of the catalyst and materials surface areas in improving the sorption kinetics and the hydrogen storage capacity.

References

[1] L. Schlapbach, A. Züttel, Nature 414 (2001) 353–358.
[2] J.A. Ritter, A.D. Ebner, J. Wang, R. Zidan, Mater. Today 6 (2003) 18–23.
[3] A. Züttel, Mater. Today 6 (2003) 24–33.
[4] G. Liang, J. Huot, S. Boily, A. Van Neste, R. Schulz, J. Alloys Compd. 292 (1999) 247–252.
[5] M. Song, J.-L. Bobet, B. Darriet, J. Alloys Compd. 340 (2002) 256–262.
[6] H. Reule, M. Hirscher, A. Weißhardt, H. Kronmüller, J. Alloys Compd. 305 (2000) 246–252.
[7] J. Huot, M.-L. Tremblay, R. Schulz, J. Alloys Compd. 356–357 (2003) 603–607.
[8] R. Janot, L. Aymard, A. Rougier, G.A. Nazri, J.M. Tarascon, J. Phys. Chem. Solids 65 (2004) 529–534.
[9] G. Liang, J. Huot, S. Boily, R. Schulz, J. Alloys Compd. 305 (2000) 239–245.
[10] G. Barkhordarian, T. Klassen, R. Bormann, J. Alloys Compd. 364 (2004) 242–246.
[11] G. Barkhordarian, T. Klassen, R. Bormann, Scripta Mater. 49 (2003) 213–217.
[12] A. Borgschulte, W. Lohstroh, R.J. Westerwaal, H. Schreuders, J.H. Rector, B. Dam, R. Griessen, J. Alloys Compd. 404–406 (2005) 699–705.
[13] G. Liang, J. Huot, S. Boily, A. Van Neste, R. Schulz, J. Alloys Compd. 297 (2000) 261–265.